Generalising the Kuramoto Model for the Study of Neuronal Synchronisation in the Brain

D.Cumin, C.P. Unsworth

The Department of Engineering Science,
The University of Auckland,
70, Symonds Street,
Auckland 1001, New Zealand.
Contact : c.unsworth@auckland.ac.nz

Keywords
Kuramoto, model, coupled oscillators, synchronisation, brain, neuron, lattice.

Abstract
In this article, we have generalised the Kuromoto model to allow one to model neuronal synchronisation more appropriately. The generalised version allows for different connective arrangements, time-varying natural frequencies and time-varying coupling strengths to be realised within the framework of the original Kuromoto model. By incorporating the above mentioned features into the original Kuromoto model one can allow for the adaptive nature of neurons in the brain to be accommodated. Extensive tests using the Generalised Kuromoto model were performed on a N=4 coupled oscillator network. Examination of how different connective arrangements, time-varying natural frequencies and time-varying coupling strengths affected synchronisation separately and in combination are reported. The effects on synchronisation for large N are also reported.

Motivation
The Kuromoto model[13][14] is a generic model used to examine the effects of synchronous behaviour in a lattice of coupled oscillators. There are regions of the brain that have been shown to be coupled and to exhibit synchronous activity as reviewed in [11]. Neuronal synchronisation also plays a role in vision [1], movement [2], memory [3] and epilepsy [4-10]. Thus, the Kuromoto model would provide a basis to modelling such phenomena of the brain. The Kuromoto model as it stands, however, describes oscillators of fixed natural frequencies, fixed coupling constants and connected together via 'all-to-all' coupling. The motivation of this work is to generalise the Kuromoto model such that it can take into account the adaptive nature of neurons and hence provide a more realistic picture of synchronisation in the brain. In order to do this, the authors have introduced time-varying natural frequencies, time-varying coupling and different connective arrangements. Results are presented for a simple lattice of 4 coupled oscillators. Examination of how different connective arrangements, time-varying natural frequencies and time-varying coupling strengths affected synchronisation separately and in combination are reported. The effect on synchronisation for large N is also reported.

1. The Kuramoto model

The generality of synchronisation from a system of oscillators was first highlighted by Winfree [12] and a mathematical model was developed which assumed the oscillators were nearly identical and that each oscillator was coupled to the collective rhythm [13].

Winfree's model was extended by Kuramoto[13][14] and simplified to equation (1)

$$\dot{\theta}_i = \omega_i + \frac{K}{N}\sum_{j=1}^{N}\sin\left(\theta_j - \theta_i\right), \quad i = 1,\ldots,N, \tag{1}$$

Where, ($d\theta_i/dt$) represents the rate of change of phase of the ith oscillator, (ω_i) is the natural frequency of the ith oscillator (distributed according to a probability density g(ω) that is unimodal and described by equation 4), K is the coupling strength, N is the number of oscillators and ($\theta_j - \theta_i$) is the difference in phases between the ith and j^{th} oscillators.

In order to visualise the synchronisation of the oscillators an order parameter, (r) was defined in [14] as:

$$re^{i\psi} = \frac{1}{N}\sum_{j=1}^{N} e^{i\theta_j} \tag{2}$$

Figure 1, shows that (ψ) is the average phase of the collection of oscillators and (r) is a measure of phase coherence of the collection of oscillators. [13] explains when r≈1 the population acts like a single oscillator and when r≈0 the individual oscillations add incoherently.

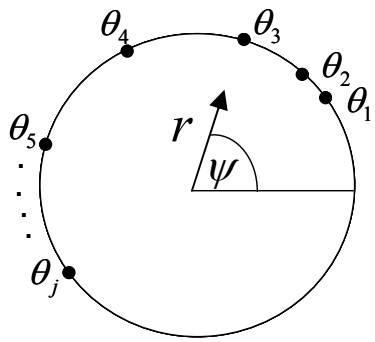

Figure 1: Visualisation of the order parameter, r.

[13] describes how synchrony occurs when (K) is above a critical value (K_c) as described by equation 3.

$$K > K_C = \frac{2}{\pi g(0)} \tag{3}$$

To illustrate the dynamics over time it is possible to display the results in a similar way to Balmforth [15] with the initial conditions being a random distribution and the natural frequencies (ω_i) chosen from a distribution g(ω) as described by equation (4):

$$g(\omega) = \begin{cases} \dfrac{(1-\omega^2)}{(\pi-2)(1+\omega^2)} & for\,|\omega| < 1 \\ 0 & for\,|\omega| > 1 \end{cases} \tag{4}$$

From equations (3) and (4), synchronisation is observed when $K_c = 0.7268$.
Figure 2 shows a numerical simulation with 500 oscillators (N=500) and K values of 0.3 (left) and 1.1 (right) to be below and above the threshold, K_c, respectively we have:

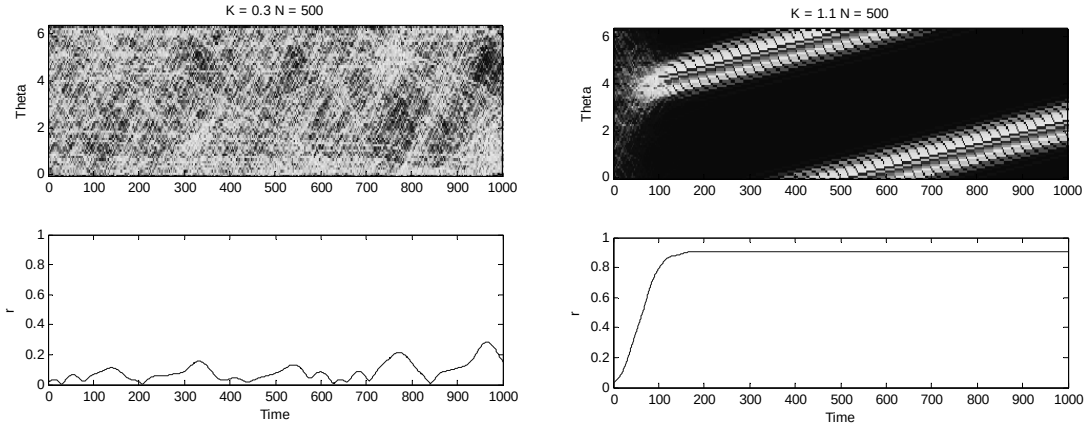

Figure 2: Comparison of the phase distribution (top) and the order parameter (bottom) for below threshold (left) and above threshold (right) values of K.

Figure 2, shows clearly how synchrony is achieved as the coupling strength (K) exceeds K_c. The below threshold case (left), has a fluctuating order parameter at low amplitude indicating that there is no coherent behaviour. The above threshold case (right), is markedly different such that within a relatively short period of time the phases of the oscillators gather together coherently and drift together. As one can see, the order parameter grows quickly, saturates and shows small fluctuations.

2. Similarities & differences of the Kuramoto model to neuronal behaviour

In the brain, the axons, or outputs, of the neurons connect via synapses to the dendrites, or inputs, of other neurons. The synapses secrete electrochemical neurotransmitter to the dendrites which can have an excitatory or inhibitory influence on the firing of the neurons they connect to [4].
From this simple representation, we can see that the Kuromoto model has some similarities and some differences to the observed behaviour in the brain. The model describes each oscillator as having a natural frequency, (ω_i). This could be seen as corresponding to the natural firing rate of a neuron [19,20]. In order, to make the Kuromoto model more realistic for synchrony in the brain one must observe that the threshold level within a neuron body can alter over time thus changing the natural firing rate of the neuron [21]. Thus, in this article we will generalise the Kuromoto model to allow for the time-varying natural frequencies. We incorporate this in the model by the inclusion of a $\omega_i(t)$ term to represent time-varying natural frequencies.
The Kuromoto model also describes the degree to which each oscillator is influenced by its neighbours from the coupling strength (K). In the brain, this could relate to the degree of excitation/inhibition that is undergone through the dendrites from neighbouring neurons to stimulate a neuron to fire. In the Kuromoto model, K, is defined to be the same for all the connections in the network and to be time-independent. However, in the brain, there is a difference such that the connection strengths can vary between neighbouring neurons depending on the usage of the dendrites and flow of neurotransmitter over time[21]. Thus, we generalise the

Kuromoto model to allow for the time-varying coupling strengths to exist between neuron(i) and neuron(j). This is incorporated into the model by the inclusion of a $K_{ij}(t)$ term to represent time-varying coupling strengths.
The Kuromoto model, assumes 'all-to-all' to coupling between oscillators. This means that each oscillator is connected to every other oscillator in the lattice. In the brain, neurons are connected in a vast number of ways. In this article, we examine the effects of different connective arrangements that could exist between 4-coupled oscillators. The connective arrangement is incorporated neatly into the model by means of the coupling strength matrix $K_{ij}(t)$. Thus a generalised form of the Kuramoto model that would be suitable to describe neuronal synchrony would be :

$$\dot{\theta}_i(t) = \omega_i(t) + \frac{1}{N}\sum_{j=1}^{N} K_{i,j}(t)\sin\left(\theta_j - \theta_i\right), \qquad i = 1,\ldots,N, \tag{5}$$

Equation 5, now allows for time-varying natural frequencies and coupling strengths to exist. In addition, the matrix $K_{ij}(t)$ allows for different connective arrangements to exist. It follows that if $K_{i,j}$ = constant and the ω_i's are fixed then the time-varying Kuromoto model of equation 5 will reduce to the static Kuramoto model of equation 1.

3. Connectivity architechures

In this article, we consider a 4 coupled oscillator system. Even for a 4 coupled oscillator system, there are many connective arrangements that one could realise. Because of this we consider 5 intuitive connective arrangements. We have defined these connective arrangements to be : 'linear unidirectional', 'linear bidirectional', 'box unidirectional', 'box bidirectional' and 'all-to-all'. Each configuration and its K_{ij} matrix are shown in Figure 3. By defining the network in this way, one can make some of the connections 0 (i.e. not connect some oscillators in one or both directions) and therefore redefine the network to realise any configuration.

$$K = \begin{bmatrix} 0 & X & 0 & 0 \\ 0 & 0 & X & 0 \\ 0 & 0 & 0 & X \\ 0 & 0 & 0 & 0 \end{bmatrix}$$

“linear unidirectional”

$$K = \begin{bmatrix} 0 & X & 0 & 0 \\ X & 0 & X & 0 \\ 0 & X & 0 & X \\ 0 & 0 & X & 0 \end{bmatrix}$$

“linear bidirectional”

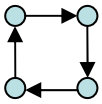

$$K = \begin{bmatrix} 0 & X & 0 & 0 \\ 0 & 0 & X & 0 \\ 0 & 0 & 0 & X \\ X & 0 & 0 & 0 \end{bmatrix}$$

“box unidirectional”

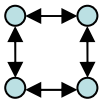

$$K = \begin{bmatrix} 0 & X & 0 & X \\ X & 0 & X & 0 \\ 0 & X & 0 & X \\ X & 0 & X & 0 \end{bmatrix}$$

“box bidirectional”

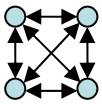

$$K = \begin{bmatrix} 0 & X & X & X \\ X & 0 & X & X \\ X & X & 0 & X \\ X & X & X & 0 \end{bmatrix}$$

“all-to-all”

Figure 3: Pictorial and matrix representation of different network models.

The next section explores the effects that different constant coupling strengths have upon the 5 different connective arrangements shown in Figure 3.

4. Constant coupling strength versus Connectivity

Figure 4, shows how the order parameter varies during 20 trials with initial phases randomly distributed in the range [0,2π] and natural frequencies chosen from the distribution described in equation (4). As mentioned in section 1, the critical coupling strength for the system is $K_c = 0.739$ [15]. Thus, we examine the effects of constant coupling strengths for the 5 connective arrangements below and above K_c, where K was chosen to be 0.3, 0.7 and 1.1. The results are shown in Figure 4.

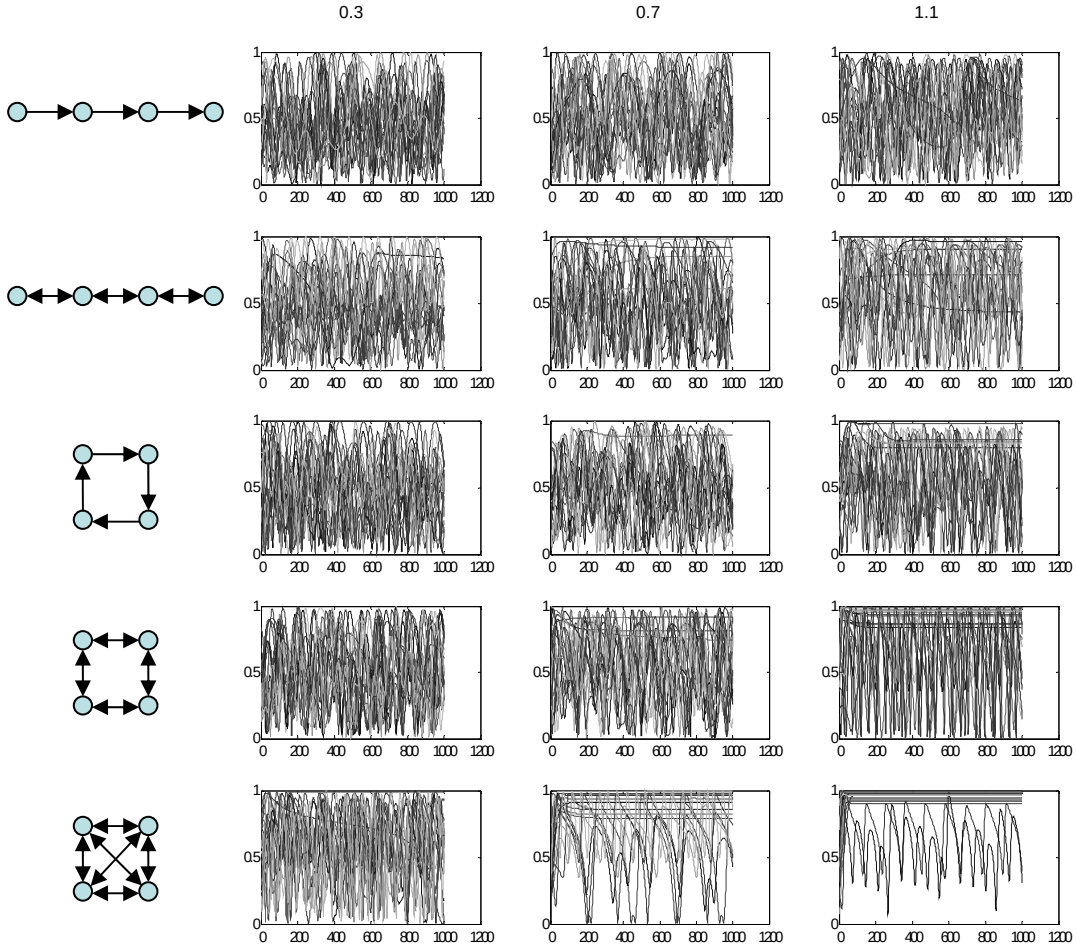

Figure 4: Variation of order parameter over time for the 5 connective arrangements for increasing constant coupling strength.

The “linear uni-directional” model of Figure 4 has the least connections and shows incoherent synchronisation as one moves from K = 0.3 to 1.1. The “linear bi-directional” model seems similar to the uni-directional case but one can see there are a few noticeable instances which produce a coherent level of synchronisation as the coupling strength increases. The “box uni-directional” model shows a few trials with strong synchronisation at the highest coupling strength of 1.1. The “box bi-directional” model shows some synchronisation occurring at K =0.7 and an increasing prominence of synchronisation at K = 1.1. Finally, the “all-to-all” model shows the most synchronisation occurring in all of the 5 arrangements. It highlights quite clearly the very strong coupling that exists at K = 0.7 and 1.1. This analysis shows how a stronger coupling strength (left to right of Figure 4) results in a greater degree of synchronisation. In addition, increasing the connectivity (i.e. the number of connections from top to bottom of Figure 4) also results in a greater the degree of synchronisation.

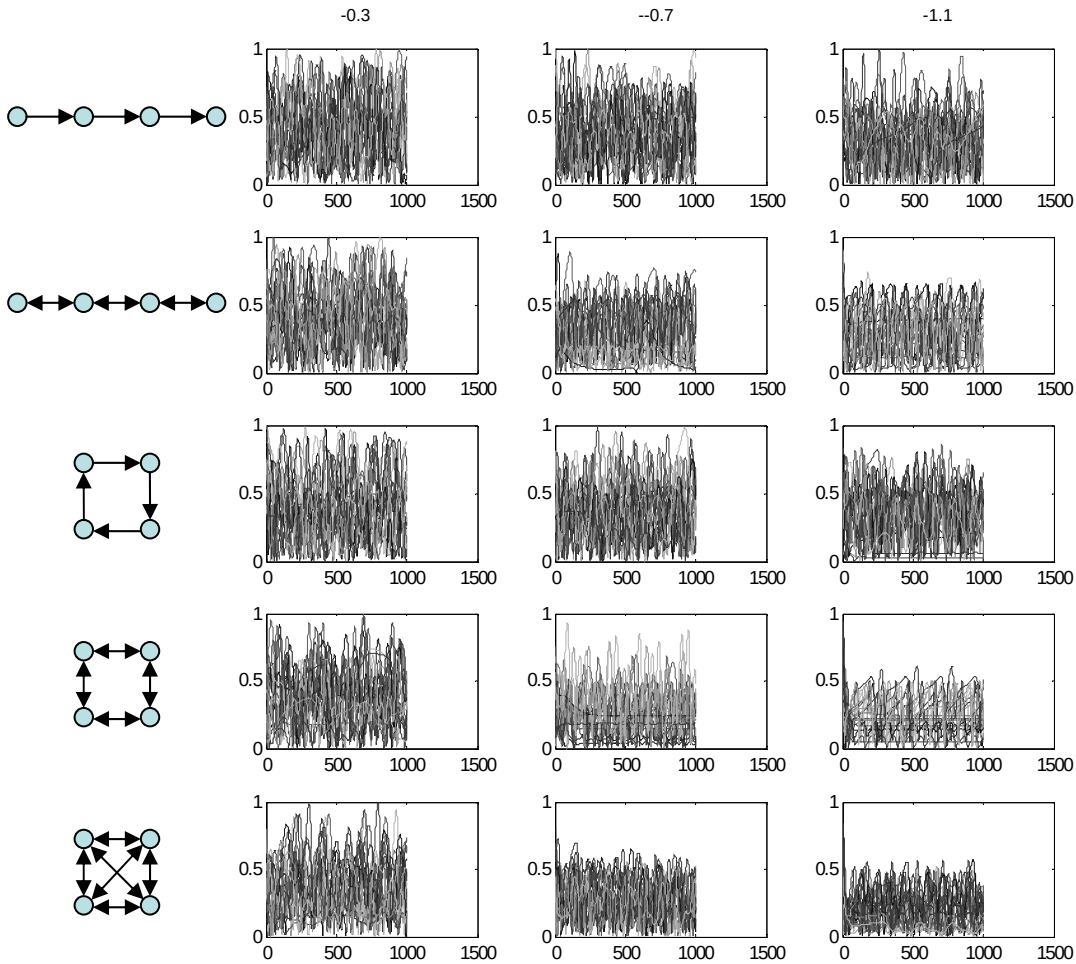

Figure 5: Negative coupling strengths. Order parameter shown over time.

Figure 5, shows how negative values of K effect the synchronisation. One can see that the negative coupling strengths serve to reduce the level of synchronisation in much the same manner as positive coupling strengths increase it, in Figure 4. The positive and negative coupling has a very interesting one to one correspondence with behaviour that occurs in the brain. The positive coupling that results in synchronisation can be likened to the effect of excitatory synapses [22]. These serve to stimulate the neurons to fire more and thus result in a higher probability of synchronisation occurring. The negative coupling that results in no synchronisation can be likened to the effects of inhibitory synapses [22]. Such synapses would serve to inhibit the neurons to fire and thus reduce the probability of synchronisation occurring. Thus, we can conclude for different connectivity and constant coupling strengths of the oscillators:

<u>For Positive Constant Coupling</u>
Increasing connectivity → Greater synchronisation
<u>For Negative Constant Coupling</u>
Increasing connectivity → Reduces synchronous

Note * :	Positive coupling maps to excitatory synapse behaviour Negative coupling maps to inhibitory synapse behaviour

This section has established the rules of how the system behaves for increasing amounts of connectivity. The investigations that follow will now be demonstrated for the 'all-to-all' case only. The reason for this, is because one can deduce from the rules established in this section what would happen for one of the 4 other connective arrangements.

5. Different Constant Coupling Strengths

In the Kuromoto model, the coupling strengths between all the oscillators were defined to have the same value K that remained independent of time. Neurons in the brain may not all be connected to the same degree. Because of this we wish to investigate how different valued coupling strengths effect synchronisation. A series of papers written by Sompolinsky [1][16] varies the coupling strength according to an average firing rate of a neuron in the visual cortex. Because the studies in [1][16] were on vision the application was constrained to a specific range appropriate for the visual problem. Whilst this study is useful in studies of vision its small dynamic range may not be indicative of general trends. Thus, we investigate the effects for a wide dynamic range of coupling strengths. We highlight this by taking a random sample of coupling strengths, K, from a normal distribution with differing means and variances for the "all-to-all" configuration. This is shown for a system with means of 0.3, 0.7, 1.1 and variances of 0.025, 0.5, 1 in Figure 6.

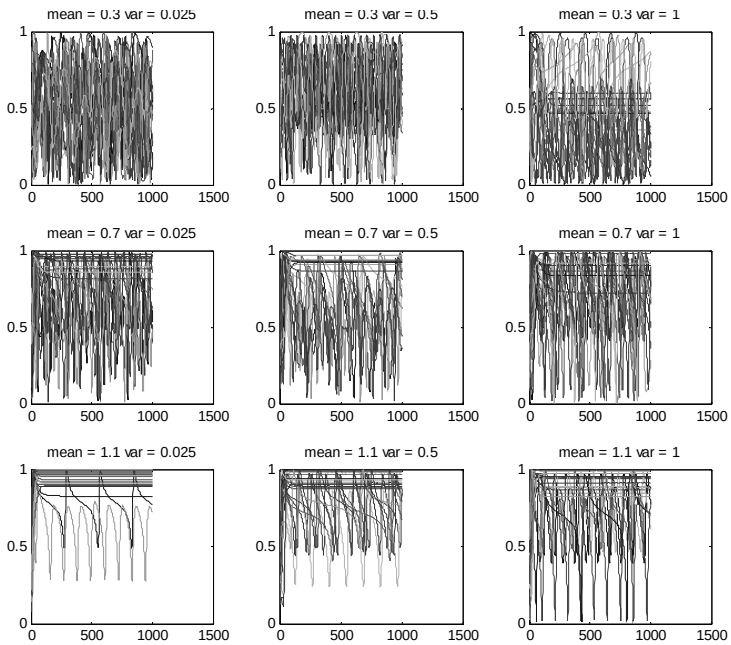

Figure 6: Variation of order parameter for different constant coupling strengths.

Figure 6, shows how the mean and variance of the coupling strengths has an effect on the order parameter. Figure 6 highlights how increasing the mean value of the K_{ij}'s produces greater synchronisation. In addition, increasing the variance of the K_{ij}'s lowers the synchronisation. Thus, the greatest synchronisation occurs when the collective mean of the oscillators' coupling strengths is large and when the collective

variance of the oscillators' coupling strength is low. Thus, we can conclude for different coupling strengths of the oscillators:

Large Mean K & Small variance of K → Greater Synchronisation
Small Mean K & Large variance of K → None Synchronous

6. Time-Varying Coupling Strength

Next we investigate the effect of how time-varying coupling strength $K_{ij}(t)$, shown in equation 5, effects the order parameter. One could choose any time-varying function for $K_{ij}(t)$. However, for the purposes of this article the authors have elected to investigate a sinusoidal time-varying function with the initial phase of each sine-wave being randomised for each oscillator. This is to allow all the K values to be visited once during the time evolution of coupling strength K of each oscillator when the time-varying coupling strength has as frequency $g_{ij} = 1$.

This has transformed equation (5) to (6) giving :

$$\dot{\theta}_i(t) = \omega_i(t) + \frac{1}{N}\sum_{j=1}^{N} K_{i,j}(t)\sin(\theta_j - \theta_i), \quad \text{for } i = 1,....,N$$
$$\text{where, } K_{i,j}(t) = \gamma + \mu\sin(2\pi g_{i,j}t + \psi_{i,j}) \qquad (6)$$

γ, μ, g_{ij} and ψ_{ij} describe the dc-offset, amplitude, frequency and phase offset respectively of the time-varying coupling strength. The frequency g_{ij} at which the coupling strength K_{ij} varies could be any positive value. For the purpose of this study, the authors have elected to normalise g_{ij} to be in the range of 0 and 1 (where 1 represents high frequencies and 0 represents low frequencies). The phase-offset, ψ_{ij}, was varied between 0-2π. In order to vary the coupling strength between 0.3 and 1.1 (namely, through the regions of interest) it was necessary to chose values of 0.7 and 0.4 for the offset and amplitude respectively. Rows 1-3 of Figure 7, show how the order parameter behaves as one moves from slow time-varying coupling strengths where the frequency $g_{ij} = 0.01$ to fast time-varying coupling strengths where $g_{ij} = 1$. In Row 4 of Figure 7, the g_{ij}*'s* have been randomised between 0-1. The columns of Figure 7, (moving from left to right) represent phase offsets ψ_{ij} (fixed at 0, fixed at π and where the phase offsets are random).

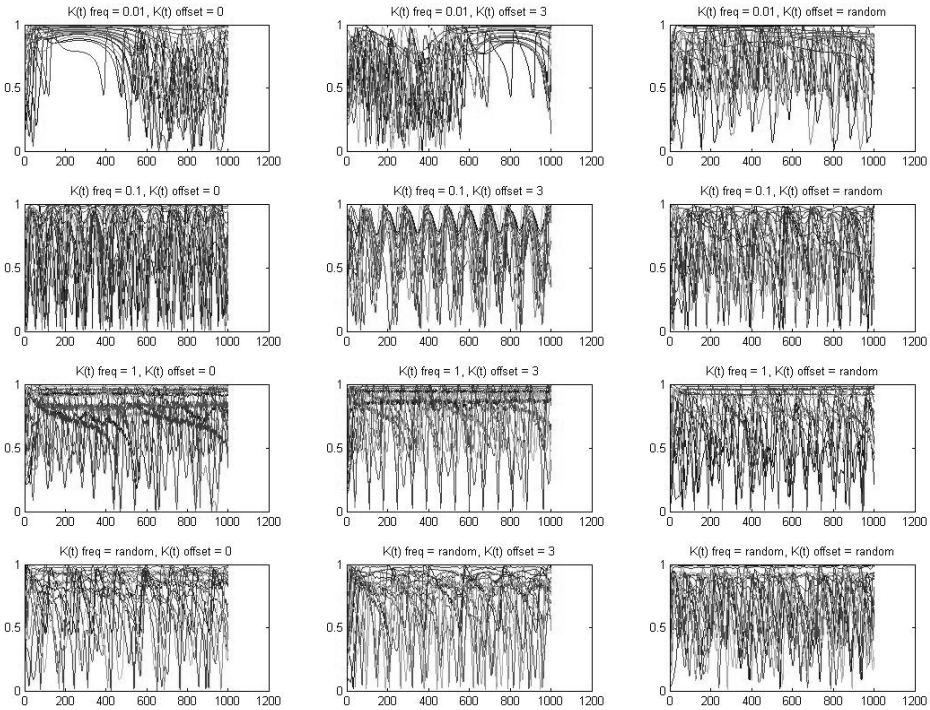

Figure 7 : The Effect of Time-Varying Coupling Strength on Order Parameter.

In the brain, the coupling strength would be governed by synaptic changes such as the diffusion of the neurotransmitter. These changes would occur over long timescales (namely slow varying changes in frequency). Thus, the first row of Figure 7 would be most likely to represent the synaptic changes in the brain. Columns 1 and 2 of row 1, show that if the K_{ij}'s all change and remain in phase with one another then synchrony occurs for high coupling strengths and dies away for low coupling strengths, as reported in section 4. Because the phase-offset is the same, the effect observed is essentially the same as keeping a high constant coupling strength which results in synchronous behaviour. Column 3 of Row 1, shows that for random phase-offsets and slow time-varying K_{ij}'s that non-synchronous activity occurs. Row 2, shows that as one increases the frequency of variation of the K_{ij}'s by a factor of 10 then the system exhibits momentary drops in and out of synchronous behaviour with a slow dropping frequency for constant phase-offsets. The authors term this 'quasi synchronisation'. The system remains non-synchronous for random phase-offsets. Row 3, shows at the highest frequency of variation of the K_{ij}'s then the system behaves in a 'quasi-synchronous' way but with a much faster dropping frequency. (Unlike in true synchronisation where the order parameter, r, remains constantly at 1, the fast fluctuations in the K_{ij}'s cause the order parameter of the system to remain at 1 but to allow the system to momentarily drop out of synchrony). This occurs even for random phase-offsets. A physical interpretation for this may be due to the fact that the variation of the K_{ij}'s is so fast the oscillators have little time to 'react' to the change in coupling strengths. Finally, Row 4, shows the effect of randomly distributing both frequency and phase-offset. Here we see non-synchronous behaviour occurring. Thus, we can conclude for time-varying coupling strengths:

<u>Slow time-varying K_{ij} with g_{ij} = constant, ψ_{ij} = constant, K large</u> → Slow Quasi Synchronisation (with large momentary drops in synchrony and a slow dropping frequency) <u>Fast time-varying K_{ij} with g_{ij} = constant, ψ_{ij} = constant, K large</u> → Fast Quasi Synchronisation (with large momentary drops in synchrony and a fast dropping frequency) <u>Time-varying K_{ij} with g_{ij} = random, ψ_{ij} = random,</u> → Non-synchronous

7. Distribution of Natural Frequencies

Before we investigate the effect of time-varying natural frequencies we would like to perform a short investigation on the distribution of natural frequencies used in the Kuromoto model. In the Kuromoto model, a unimodal distribution of natural frequencies was used as described by equation 4. In the generalised model, proposed here, we wish to investigate how synchronisation is effected by the type of distributions used to represent the natural frequencies. There are a whole host of distributions one could use. The authors elected to investigate two of the most widely used distributions. These are the 'Gaussian distribution' and the 'Uniform distribution' [23]. The synchronisation was observed over 20 trials were the natural frequencies were randomly chosen from a range of Gaussian distributions of means of 0, 0.5, 1 and variances of 0.125, 0.5, 1, shown in Figure 8. Similarly, synchronisation was observed for a range of uniform distributions with ranges 1, 4 and 8, shown in Figure 9. Figures 8 and 9 used all-to-all coupling with K= 0.7. For the Gaussian distribution it was found that the mean of the distribution did not affect synchronisation. For both distributions, we found good agreement with Winfree's discovery [12] that when the variance of natural frequencies is large, the synchronisation is severely decreased. Thus, we can conclude for the two most commonly distributions:

<u>Gaussian Distribution</u>		
Varying the Mean	→	Does not affect synchronisation
Decreasing the variance	→	Increases Synchrony
<u>Uniform Distribution</u>		
Decreasing the Range	→	Increases Synchrony

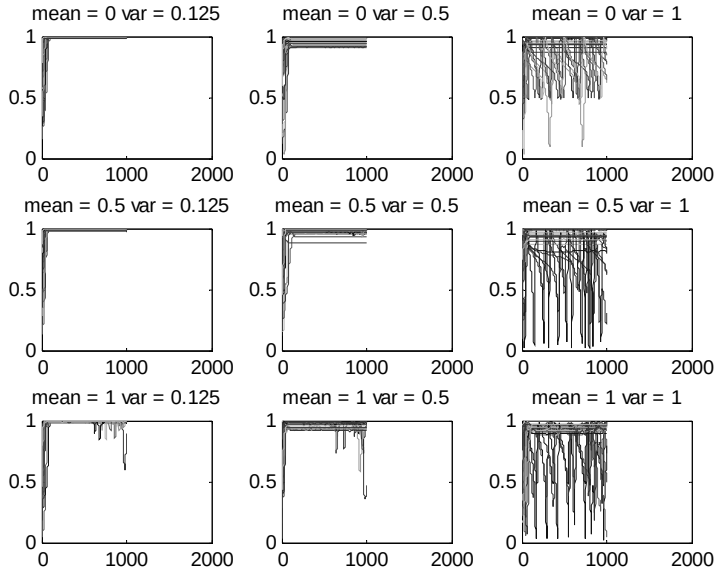

Figure 8: Natural frequencies taken from Gaussian distributions of means (0, 0.5, 1) and variances (0.125, 0.5).

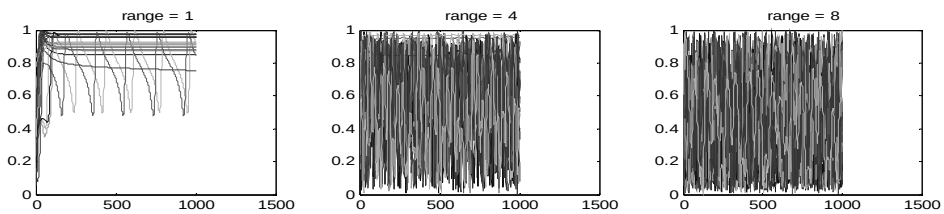

Figure 9: Natural frequencies taken from Uniform distributions with ranges (1,4,8)

8. Time-Varying Natural Frequencies

In the Kuromoto model, the natural frequencies of the oscillators remain constant over time. As mentioned earlier, to make the Kuromoto model realistic for synchrony in the brain one must observe that the threshold level within a neuron body can alter over time thus changing the natural firing rate of the neuron [21]. Thus, the natural frequency can be time-varying, ω_i(t). As in the time-varying coupling strengths of section 6, one could choose any time-varying function for ω_i(t). As in section 6, we have allowed for the natural frequency (f_i) to be normalised between 0 and 1 and to vary sinusoidal with an initial phase-offset (φ_i). To describe this behaviour the time-varying natural frequency equation becomes (7):

$$\omega_i(t) = \alpha_i + \beta_i \sin(2\pi f_i t + \varphi_i) \qquad (7)$$

Thus, to allow all the natural frequencies to be visited once in single cycle for $f_i = 1$, we set $\alpha_i = \beta_i = 0.5$. Figures (10-12), show the effect of time-varying natural frequencies for constant coupling strengths of K = 0.3, 0.7 and 1.1.

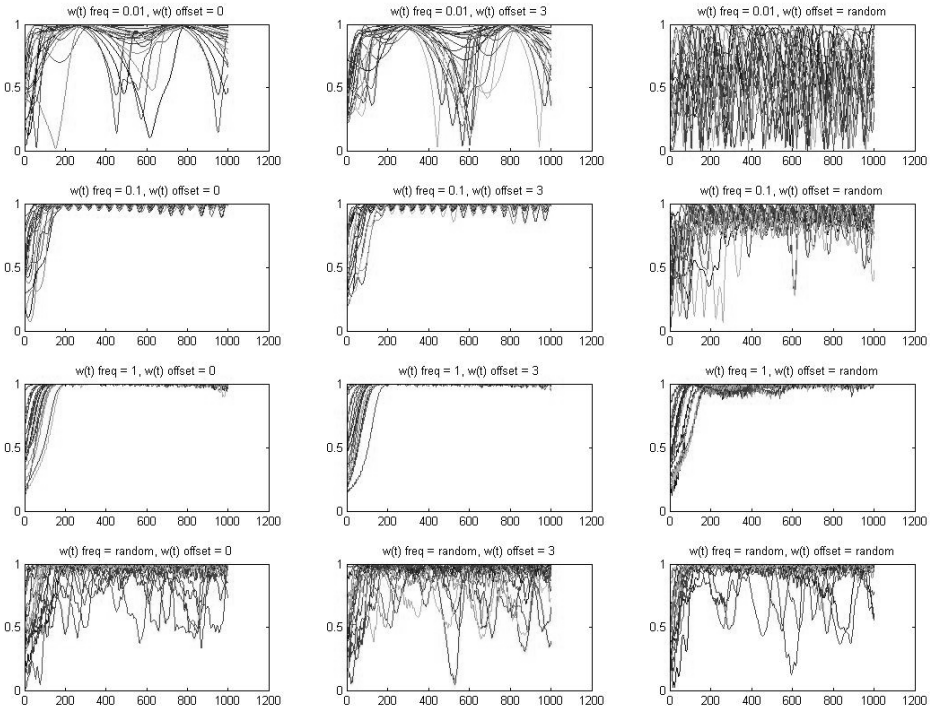

Figure 10 : Effect of time-varying natural frequencies for K=0.3

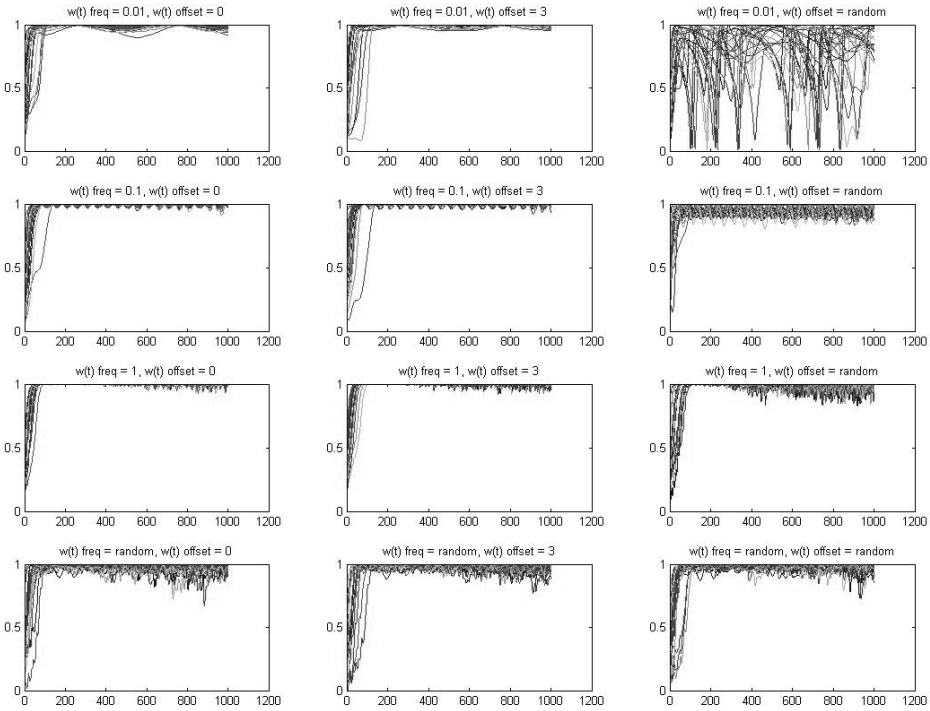

Figure 11 : Effect of time-varying natural frequencies for K=0.7

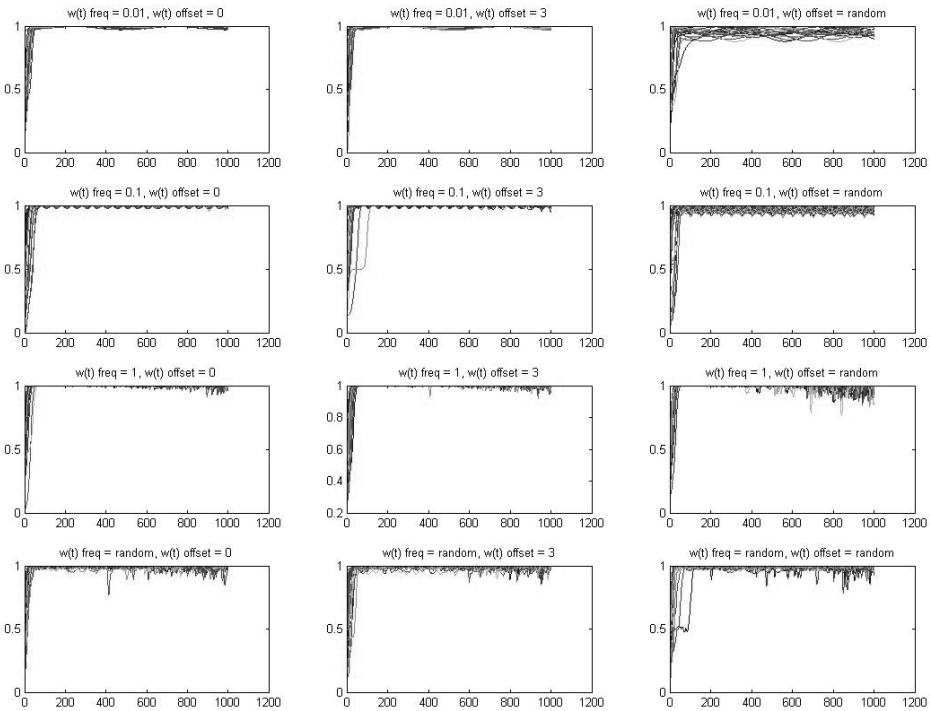

Figure 12 : Effect of time-varying natural frequencies for K=1.1

Figure 10 shows a very similar result to the time-varying coupling strengths of section 6. However, the effect of the natural frequencies is more dominant than that of the coupling strengths. The second row highlights quite nicely that as the natural frequency increases the system oscillates in and out of a strong synchrony producing a similar 'quasi synchronous' state with small momentary drops in synchrony, as opposed to the large momentary drops in synchrony observed in the time-varying coupling strengths. The quasi-synchrony produced here is much stronger than the quasi-synchrony of Figure 7. In addition, the momentary drops in synchrony are much smaller than those observed in Figure 7 for time-varying coupling. The third row shows, even when the coupling is low, that if the frequency is high, the frequency dominates and forces a strong synchronous effect to be observed (even for random phase offsets). The fourth row, shows that synchrony decreases for randomly generated frequencies.
Figures 11 and 12, show a consistent increase in synchrony as the coupling strength is increased. Thus, we can conclude for time-varying frequencies for fixed coupling strengths:

<u>Slow time-varying ω_i with constant small K</u>
→ Slow Quasi Synchronisation
(with small momentary drops in synchrony and slow dropping frequency)

<u>Fast time-varying ω_i with constant large K</u>
→ Fast Quasi Synchronisation occurs
(with small momentary drops in synchrony and fast dropping frequency)

Note * : The natural frequencies dominate synchrony more than coupling strength.

9. Time-Varying Coupling Strengths & Time-Varying Natural Frequencies

Combining the time varying effects of both coupling strength and natural frequencies, we derive equation 8:

$$\dot{\theta}_i(t) = \omega_i(t) + \frac{1}{N}\sum_{j=1}^{N} K_{i,j}(t)\sin(\theta_j - \theta_i) \qquad \text{for } i = 1,....,N \qquad (8)$$

$$\text{where, } \omega_i(t) = \alpha_i + \beta_i \sin(2\pi f_i t + \varphi_i) \quad \text{and} \quad K_{i,j}(t) = \gamma + \mu \sin(2\pi g_{i,j} t + \psi_{i,j})$$

Figure 13-15 shows all the permutations for a very slow time-varying coupling strength of frequency (g_{ij}= 0.01 and random) and phase offset (ψ_{ij} = 0 and random) for very slow, slow and fast time-varying natural frequencies of (f_i = 0.01, 0.1, 1) and phase offsets (φ_i = 0 and random).

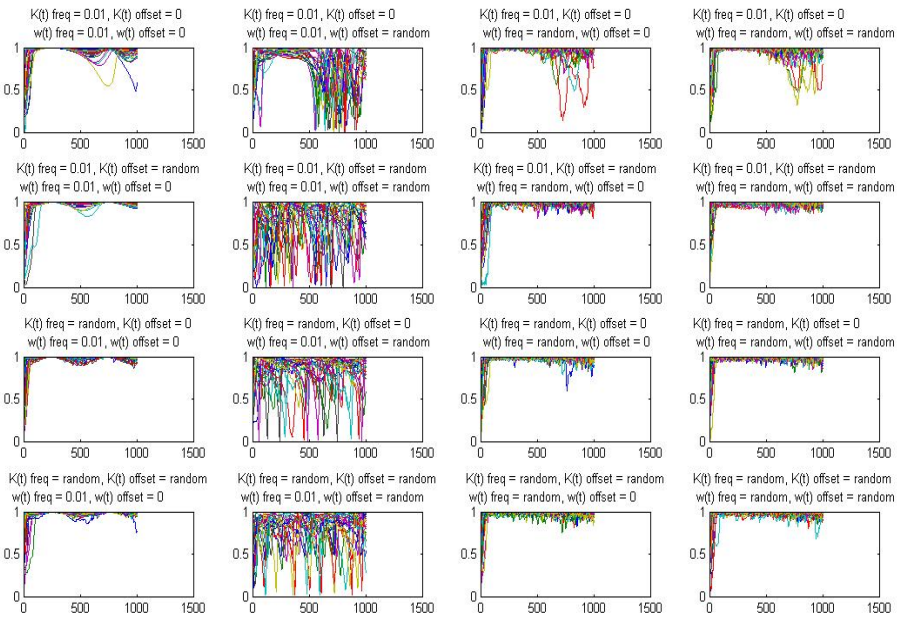

Figure 13 : Very slow time-varying coupling strengths & very slow time-varying natural frequencies

The 1st & 2nd column of Figure 13, show that for very slow varying coupling strengths (f_i =0.01) and very slow varying natural frequencies (g_{ij} =0.01) that the phase offset of the natural frequencies is crucial for synchrony to occur. Column 3, shows how the system still manages to retain high synchrony as long as the phase offset of the natural frequencies is constant. Column 4, (and especially the 4th row of the column) highlights a very interesting form of behaviour. This is when all the time-varying frequencies are randomly chosen and the offsets are randomly chosen then one observes a synchronous behaviour with small random fluctuations in synchrony. We will discuss this further at the end of the section.

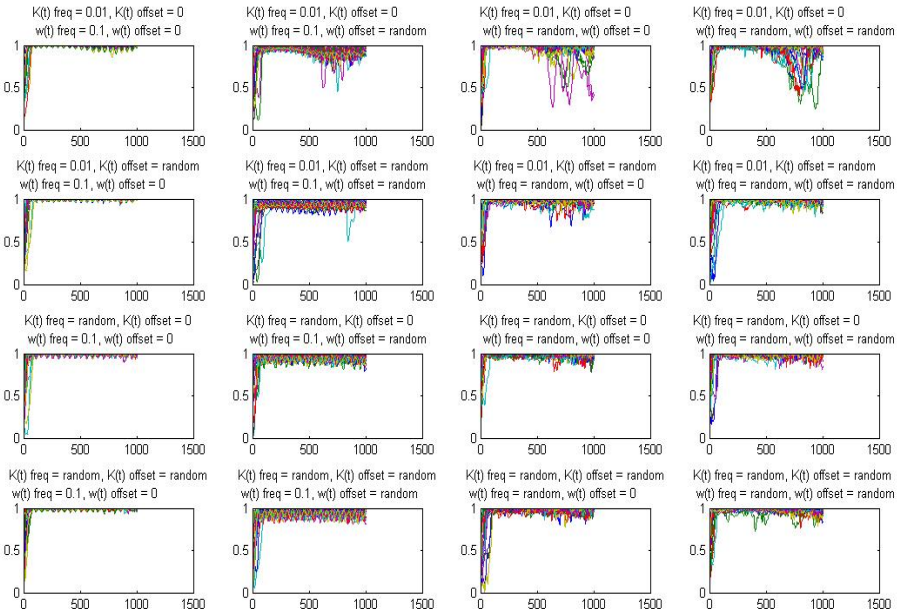

Figure 14 : Very slow time-varying coupling strengths & slow time-varying natural frequencies

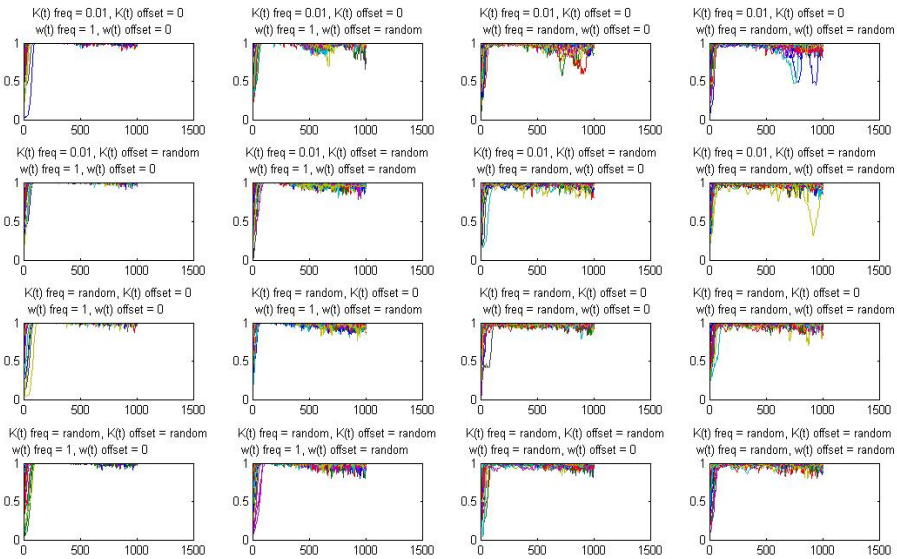

Figure 15 : Very slow time-varying coupling strengths & fast time-varying natural frequencies

Figures 14 and 15, show that as the time-varying natural frequencies increase then the fast varying frequencies dominate and produce high levels of synchrony.

Figure 16-18, shows the permutations for combined effect for a fast time-varying coupling strength of frequency (f_{ij}= 1 and random) and phase offset (ψ_{ij} = 0 and random) for very slow, slow and fast time-varying natural frequencies of (ω_i = 0.01, 0.1, 1) and phase offsets (φ_i = 0 and random).

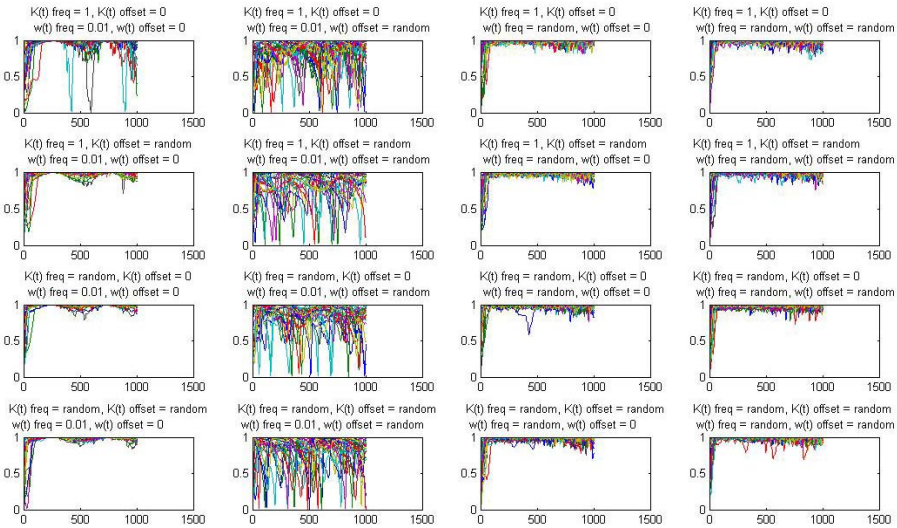

Figure 16 : Fast time-varying coupling strengths & very slow time-varying natural frequencies

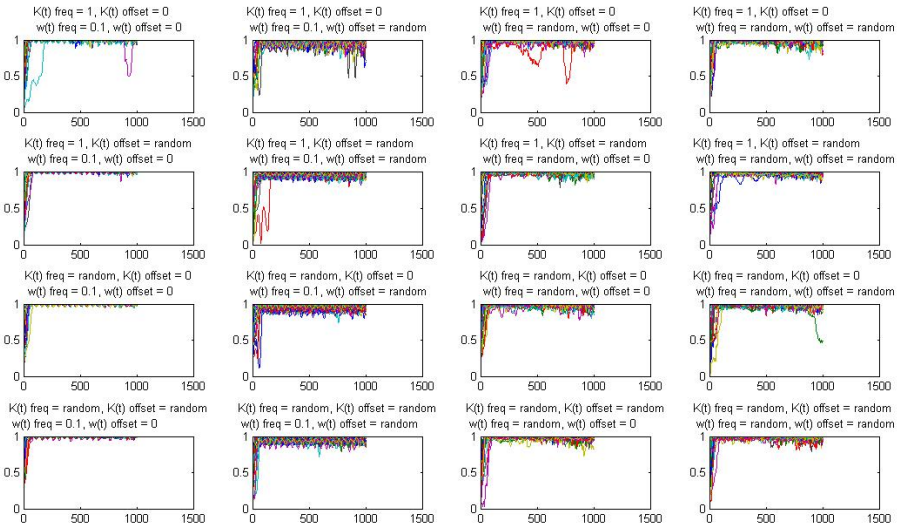

Figure 17 : Fast time-varying coupling strengths & slow time-varying natural frequencies

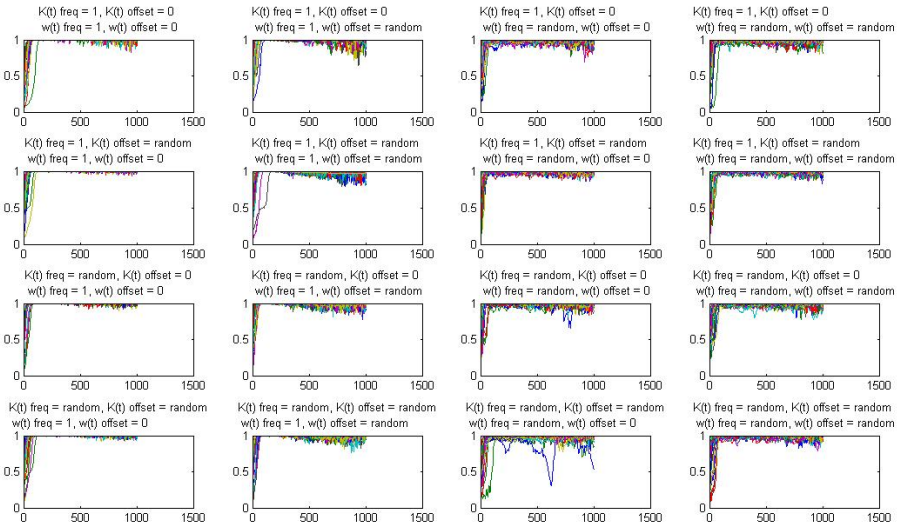

Figure 18 : Fast time-varying coupling strengths & fast time-varying natural frequencies

As one can see, high levels of quasi synchrony occur in Figures 16-18 and quasi synchrony increases as the frequency of the time-varying natural frequencies increases.

As mentioned earlier, the bottom left plot of each of the Figures 13-18 presents an interesting result that is non-intuitive. It seems that by randomly choosing the initial frequencies and phase-offsets of the time-varying coupling strengths and natural frequencies that the system as a whole produces high quasi synchrony with small random fluctuations in the synchrony. In order to address this we must first remind ourselves that the results obtained were for 4 oscillators in the all-to-all configuration. We now ask the question does the coupling arrangement and the number of oscillators have an effect on the synchrony of the system. We examine this in sections 9.1 and 9.2 below.

9.1 Altering the connectivity

As reported in section 3, on connectivity, one would expect the system to lose synchrony by reducing the connectivity. However, in the previous results we did not examine time-variation effects. We thus, repeat the results for the 5 different connective arrangements of 4 oscillators for time-varying natural frequencies and coupling strengths, shown in Figures 19-23.

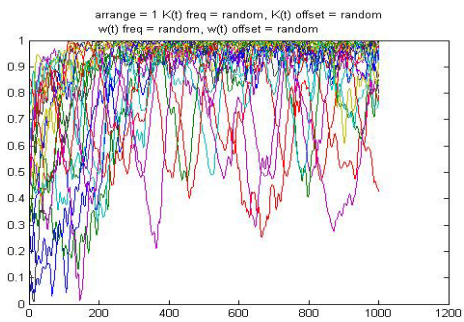

Figure 19 : Linear Unidirectional

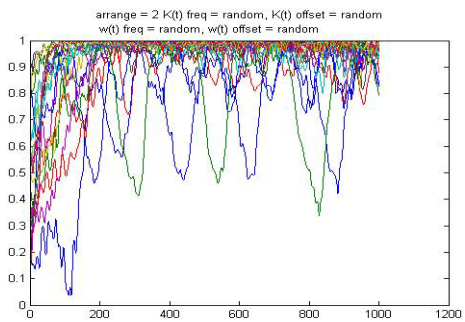

Figure 20 : Linear Bidirectional

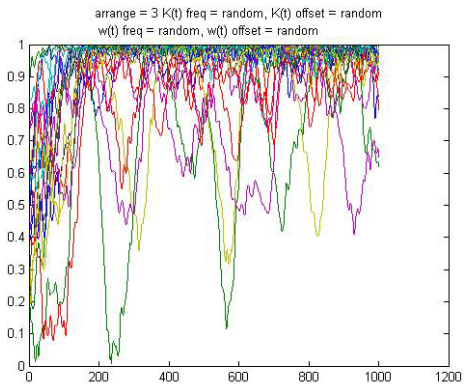

Figure 21 : Box Unidirectional

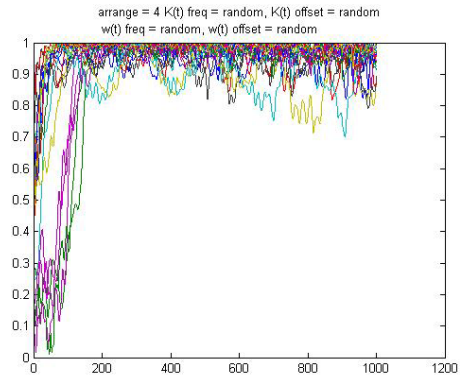

Figure 22 : Box Bidirectional

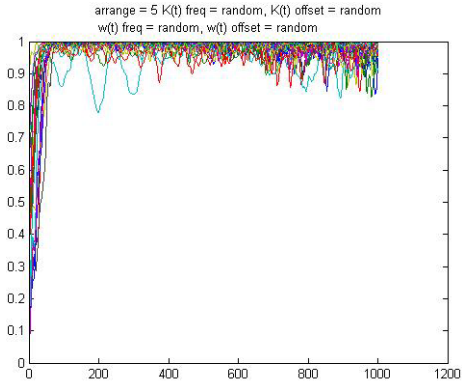

Figure 23 : All-to-All

Figures 19-23, show that the type of connectivity used does alter the synchrony in the same manner as we reported in section 3 for the non time-varying case.
Thus, the high quasi synchronous behaviour is a consequence of the 'all-to-all' connective arrangement only (Figure 23) and the quasi synchrony reduces as the amount of connectivity reduces (Figures 19-22). Although we have established that 'all-to-all' arrangement is responsible for the high quasi synchrony it is necessary to understand why it is occurring in this case. By performing a short examination of how the number of oscillators used in the network effects synchrony we can deduce the reason for high quasi synchrony in the 'all-to-all' case.

9.2 Increasing the number of oscillators

The same experiment with random time-varying frequencies and coupling strengths and random phase offsets was performed using an 'all-to-all' configuration for 50 and 500 connected oscillators. The results of which are shown in Figures 24-25 respectively.

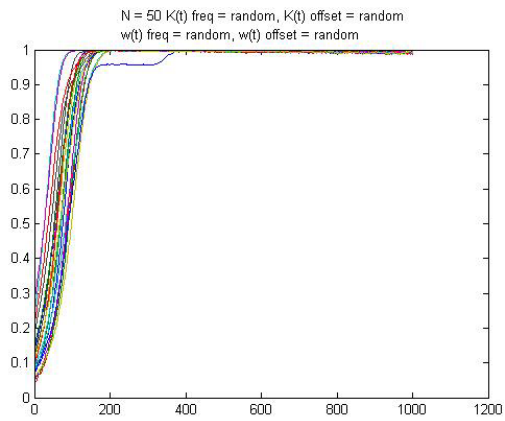

Figure 24 : N = 50

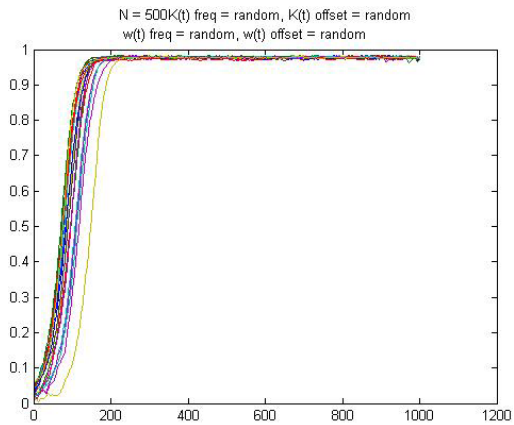

Figure 25 : N = 500

By comparing Figures 23-25, we see that increasing N from 4 to 500 moves the network from quasi synchronous (Figure 23) to synchronous behaviour (Figure 25). One also observes the logical result that it takes longer for the 500 oscillators (in Figure 25) to obtain synchrony than the 50 oscillators (in Figure 24).
The number of oscillators is also associated with the connectivity of the network. Namely, as oscillators increase the connectivity of the network increases (e.g. In Figure 25, for 'all-to-all' coupling each oscillator has 1000 connections to rest of the network. Thus, there is a higher likelihood that the individual oscillators will be

influenced by the network and will reduce to some mean level of vibration and hence become synchronous. In comparison, Figure 23, has only 12 connections for an oscillator. Thus, the network has less influence on the individual oscillators in the N=4 case and thus there is a smaller likelihood that the network will change the individual behaviour of the oscillators. Thus, we observe the random fluctuations in the order parameter for N=4). This is highlighted quite nicely, by looking at the phase distribution of Figures 26-28 that correspond to Figures 23-25 respectively for single trials. Here we observe that the 'all-to-all' connectivity even at 4 oscillators produces a quasi-in-phase behaviour.

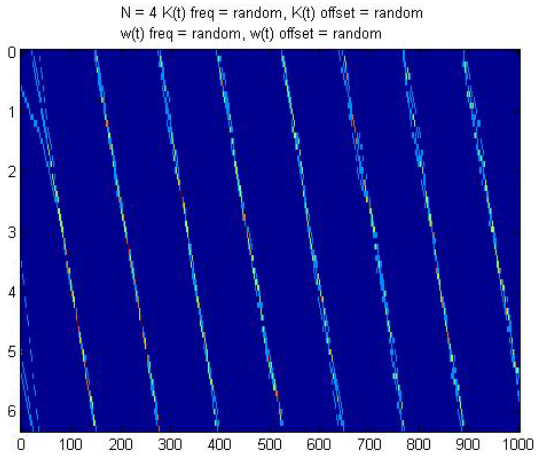

Figure 26 : Phase distribution for N=4, random time-varying parameters

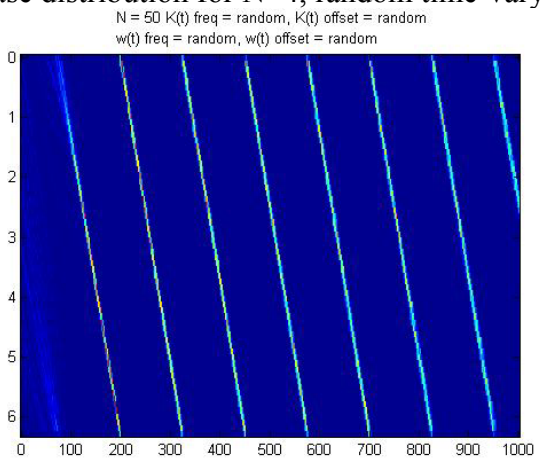

Figure 27 : Phase distribution for N=50, random time-varying parameters

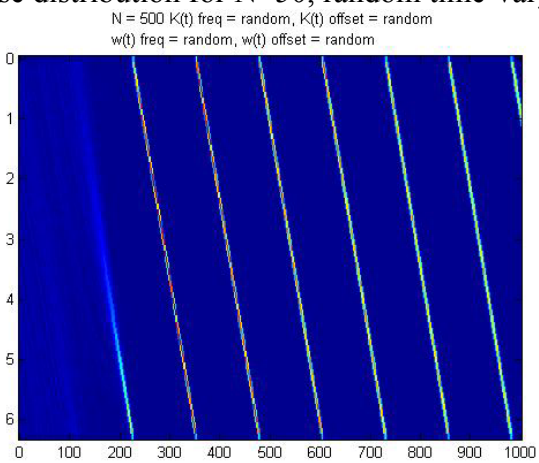

Figure 28 : Phase distribution for N=500, random time-varying parameters

Also we see that the oscillators are randomly fluctuating but such is the high connectivity of the system that the system forces them to align to produce a quasi-in-phase behaviour. As N increases the quasi-in-phase behaviour tends to in-phase behaviour and synchrony and it takes longer for the system to synchronise. Thus, the connective arrangement of the 'all-to-all' coupling, even when N=4 and is small, is strong enough to produce a strong quasi-synchronous behaviour when both the natural frequencies and coupling strengths are time-varying. Thus, we can conclude for time-varying frequencies and time-varying coupling strengths:

<u>For 'all-to-all' (high connectivity), Low N</u>
<u>Very slow time-varying f_i and very slow time-varying g_{ij}</u>
→ quasi synchrony dependent on φ_i is constant
(with slow dropping frequency)

Increasing time-varying f_i for slow time-varying g_{ij}
→ Increases quasi synchrony
(with increasing dropping frequency)

<u>Very slow time-varying f_i and fast time-varying g_{ij}</u>
→ quasi synchrony dependent on φ_i is constant
(with slow dropping frequency)

Increasing time-varying f_i for fast time-varying g_{ij}
→ Increases quasi synchrony
(with increasing dropping frequency)

<u>Randomly generated initial f_i, g_{ij}, φ_i and ψ_{ij}</u>
→ quasi synchrony
(with small random fluctuations)

<u>As connectivity decreases, Low N</u>
→ Randomness increases

<u>For 'all-to-all' (high connectivity), Increase N</u>
→ synchrony occurs
(and takes longer as N increases)

Conclusions

A 'Generalised Kuromoto model to study the effects of neuronal synchrony' was developed and extensive tests using a N=4 coupled oscillator network were performed. Examination of how different connective arrangements, time-varying natural frequencies and time-varying coupling strengths affected synchronisation separately and in combination were reported. The effects on synchronisation for large N were also reported.

In the Kuromoto model, 'all-to-all' coupling between oscillators is assumed. In the brain, neurons are connected in a vast number of ways. Thus, we incorporated a coupling strength matrix, K_{ij}, in the original Kuromoto model to allow for any type of connective arrangement to exist. For the N=4 system, constant coupling strength

versus 5 intuitive connective arrangements was examined. Synchronisation was found to increase for increasing connectivity for positive constant coupling. Negative constant coupling was also explored and found to reduce synchrony for increasing connectivity. Positive coupling was found to map to the excitatory synapse and negative coupling to the inhibitory synapse in the brain.

In the Kuromoto model, the coupling strength, K, was defined to be the same for all the connections in the network. In the brain, the connection strengths could be different between neighbouring neurons. The $K_{i,j}$ matrix introduced allows for different coupling strengths to be realised also. Experiments for different coupling strengths were investigated for N=4. It was found that when mean coupling strength of the oscillators in the lattice is large and the variance of the coupling strength is small then synchrony is achieved. The converse was also found to be true.

In the Kuromoto model, the coupling strength, K, was also time-independent. However, in the brain the coupling strengths can vary with time and thus are time-dependent. Thus, time-varying coupling strengths were incorporated into the original model by allowing the $K_{i,j}$ matrix to be a function of time, namely $K_{i,j}(t)$. The time-varying function of the coupling strength was chosen to be sinusoidal. The effects of time-varying coupling strength was examined for constant natural frequencies. It was found that slow time-varying coupling strengths with constant frequency and constant phase gave a slow quasi-synchronisation as the coupling strength became large. The quasi-synchrony was described to have large momentary drops in synchrony and a slow dropping frequency. As the frequency of the time-varying coupling strength was increased faster quasi-synchronisation with faster dropping frequency resulted. It was found that when the frequency and phase of the time-varying coupling strength was random for constant natural frequencies that non-synchronous behaviour resulted.

In the Kuromoto model, a single distribution was used to choose the natural frequencies from, described by equation 4. In the brain, the natural firing of the oscillators may come from a very different distribution. Thus, for completeness, we decided to investigate two common types of distribution (namely the Gaussian and Uniform distribution). It was found that if the natural frequencies were drawn from the Gaussian distribution that varying the distributions mean did not affect synchrony but decreasing the variance of the distribution served to increase synchrony. For the Uniform distribution it was found that by decreasing the range increased the synchrony.

In the Kuromoto model, the natural frequencies of the oscillators were defined to have frequencies that were time-independent. In the brain, the frequency of the neurons firing can vary over time and is thus time-independent. This was incorporated into the original Kuromoto model by allowing for a $\omega_i(t)$ term to represent time-varying natural frequencies. The time-varying function of the natural frequencies was chosen to be sinusoidal. The effects of time-varying natural frequencies with constant coupling strengths were then investigated. It was found that slow time-varying natural frequencies with small constant coupling strengths produced a slow quasi-synchronisation with small momentary drops in synchrony and slow dropping frequency. This effect increased as the time-varying natural frequency was increased for constant large coupling strengths. It was observed that the time-varying natural frequencies produced stronger synchronisation effects than those produced by the time-varying coupling strengths.

Finally, the effect of combining both time-varying natural frequencies and time-varying coupling strengths together was examined by incorporating both $\omega_i(t)$ and $K_{i,j}(t)$ into the original Kuromoto model. Both $\omega_i(t)$ and $K_{i,j}(t)$ were chosen to be

sinusoidal. It was observed that for very slow time-varying natural frequencies and very slow varying coupling strengths that quasi-synchrony occurred with slow dropping frequency. The quasi-synchrony was dependent on the phase of the natural frequencies being constant. By increasing the time-varying natural frequency it was found that the quasi-synchrony increased with increasing dropping frequency. Similar results were found for very slow time-varying natural frequencies and fast time-varying coupling strengths. It was found when the time-varying natural frequencies and coupling strengths and their phases were initially randomly chosen that quasi synchrony occurred with small random fluctuations. Upon further investigation if was found that this was a consequence of the 'all-to-all' connective arrangement used and that the quasi-synchrony reduced to randomness as the connectivity decreased. It was also shown that when both the natural frequencies and coupling strengths and their phases were randomly chosen that the 'all-to-all' arrangement was strong enough, even at small numbers of oscillators N=4, to force quasi-synchronous behaviour. In addition, by increasing the number of oscillators to N=500 it was shown that the quasi-synchrony observed in the N=4 case was forced to become synchronous for higher numbers of oscillators. It was also observed that the more oscillators used in the network causes the network to take longer to produce synchrony in the time-varying case. The results also demonstrate that when separate effects were combined that a superposition of the effects would occur.

In this article, we have generalised the Kuromoto model to allow one to model neuronal synchronisation more appropriately. The generalised version allows for different connective arrangements, time-varying natural frequencies and time-varying coupling strengths to be realised within the framework of the original Kuromoto model. By incorporating the above mentioned features into the original Kuromoto model one can allow for the adaptive nature of neurons in the brain to be accommodated.

Acknowledgements

The work was supported by the University of Auckland Research Council Grant scheme.

References

1. Sompolinsky, H., Golomb, D., Kleinfeld, D., Cooperative dynamics in visual processing. Physical Review A, 1991. 43(12): p. 6990 - 7011.
2. Cassidy, M., Mazzone, P., Oliviero, A., et al, Movement-related changes in synchronisation in the human basal ganglia. Brain, 2002. 125(6): p. 1235 - 1246.
3. Klimesch, W., Memory processes, brain oscillations and EEG synchronisation. International Journal of Psychophysiology, 1996. 24(1-2): p. 61 - 100.
4. Kandel, E.R., Schwartz, J.H., Jessell, T.M., Principals of neural science. 3 ed. 1991, Norwalk, CT: Appleton and Lange.
5. Traub, R.D., Wong, R.K., Cellular mechanisms of neural synchronisation is epilepsy". Science, 1982. 216: p. 745 - 747.
6. Engel, J., Pedley, T.A., Epilepsy: A Comprehensive Text-book. 1997, Philadelphia: Lippincott-Raven.
7. Lehnertz, K., Non-linear time Series Analysis of Intracranial EEG Recordings in Patients with Epilepsy - an Overview". International Journal of Psychophysiology, 1999. 34: p. 45 - 52.

8. Mormann, F., Lehnertz, K., David, P., Elger, C.E., Mean phase coherence as a measure for phase synchronization and its application to the EEG of epilepsy patients. Physica D, 2000. 144: p. 358 - 369.
9. Lopes das Silva, F.H., Suffczynski, P., Parra, J. et al, Epilepsies as Dynamic Diseases of Brain Systems: Basic Models and the Search for EEG/Magnetoencephalography (MEG) Signals of Impending Seizures. Epilepsia, 2001. 42(suppl. 7): p. 3.
10. Varela, F.J., The Preictal State: Dynamic Neural Changes Preceding Seizure Onset. Epilepsia, 2001. 42(suppl. 7): p. 3.
11. Bennet, M.V.L., Zukin, R.S., Electrical Coupling and Neuronal Synchronisation in the mammalian Brain. Neuron, 2004. 41: p. 495 - 511.
12. Winfree, A.T., Biological rhythms and the behavious of populations of coupled ossilators. Journal of Theoretical Biology, 1967. 16: p. 15.
13. Strogatz, S.H., From Kuramoto to Crawford: exploring the onset of synchronization in populations of coupled oscillators. Physica D, 2000. 143: p. 1 - 20.
14. Kuramoto, Y., Arakai, H., Chemical Oscillations, Waves and Turbulence. 1984, Berlin: Springer.
15. Balmforth, N.J., Sassi, R., A shocking display of synchrony. Physica D, 2000. 143: p. 21 - 55.
16. Sompolinsky, H., Golomb, D., Kleinfeld, D., Global processing of visual stimuli in a neural network of coupled oscillators. Proceedings of the National Academy of Sciences U.S.A., 1990. 87(18): p. 7200-7204.
17. Köhling, R., GABA Becomes Exciting. Science, 2002. 298(5597): p. 1350 - 1351.
18. Lee, S.H., Magge, S., Spencer, D.D., Sontheimer, H., Cornell-Bell, A.H., Human epileptic astrocytes exhibit increased gap junction coupling. Glia, 1995. 15(2): p. 195 - 202.
19. Llinas, R.R., The Intrinsic Electrophysiological Properties of Mammalian Neurons. Science, 1988. 242(4886): p. 1654 - 1664.
20. Hutcheon, B., Yarom, Y., Resonance, oscillation and the intrinsic frequency preferences of neurons. Trends in Neural Science, 2000. 23(5): p. 216 -222.
21. Principles of Neural Science (2nd Edition), Editors E.R Kandel and J.H.Schwartz, Elsevier 1985, New York.
22. Fundamentals of Computational Neuroscience, T. Trappenberg, Oxford University Press, 2002, UK, pp 19-21.
23. Probability, Random Variables & Stochastic Processes, A. Papoulis, Third Edition, McGraw Hill, 1991, pp 74-75.
24. High frequency (600Hz) SEP activities origination in the subcortical and cortical human somatosensory system, R.Gobbele, H.Buchner et.al.,Electroenceph. Clin. Neurophysiol, vol.108, 1998, pp. 182-9.